

## Numerical eigenstates for a two-antidot channel under a magnetic field

B. L. Johnson, P. B. Kohl, and D. M. Retzlaff

*Department of Physics and Astronomy, Western Washington University, Bellingham, Washington, 98225*

(Received 14 March 2002; published 17 October 2002)

We have calculated the single-particle eigenstates of a system designed to model a two-dimensional channel obstructed by a pair of anti-dots, under a transverse magnetic field. The model is relevant to recent experiments in which the conductance of the two-antidot system reveals a conductance minimum which is modulated by oscillations of a *constant period in a magnetic field*, contrary to the predictions of semiclassical calculations. We show that the modulations are due to the evolution with applied magnetic field of the eigenstates occupying the Fermi level, which alternate between cyclotron resonant states and states which are pinched off in the constricted region between the antidots and the channel edge. The phenomenon is an example of the interplay of the semiclassical cyclotron behavior and the quantum-mechanical nature of the constrictions.

DOI: 10.1103/PhysRevB.66.153311

PACS number(s): 73.23.-b, 73.63.-b

The study of electron transport in semiconductor devices of reduced dimensionality has been of great recent interest. In particular, systems at very high magnetic fields,<sup>1</sup> or systems at very low magnetic field have been studied extensively.<sup>2</sup> These represent distinct regimes: the latter is often treated via semiclassical ballistic trajectories, while the former is described via well-defined quantum mechanics of Landau levels. The crossover region between these regimes has been difficult, due in large part to the difficulty in designing and performing appropriate experiments (and corresponding theoretical models) which isolate the crossover regime in a clear fashion.

A recent experiment<sup>3</sup> designed to probe the crossover region has produced some interesting results; interpretation of the experiment has been difficult, and no clear picture has emerged.<sup>4-7</sup> The device of interest consists of a quantum wire of two-dimensional electron gas, with a pair of antidots situated side by side obstructing the channel (see Fig. 1). The most important features of this device are the two narrow constrictions separating the channel edges from the antidots. In the experimental setup, the wire width is  $2\ \mu\text{m}$ , while the dot diameters (lithographically) are  $0.2\ \mu\text{m}$ . The two-terminal conductance of the device as a function of applied (perpendicular) magnetic field is shown in Fig. 2(a); note that the conductance shows a prominent dip, modulated by Anharinov-Bohm oscillations, centered at a magnetic field of roughly  $0.23T$ . For the experimental parameters, the field where the broad dip in conductance occurs corresponds to an electron cyclotron orbit which just fits the channel, enclosing the two antidots (shown schematically in Fig. 1). The loss of conductance corresponds to the trapping of electrons in this cyclotron orbit. The Aharonov-Bohm (AB) oscillations are due to quantum interference associated with the multiply connected geometry, i.e., states transmitted through the constrictions, and the trapped cyclotron states. Remarkably, the period of these AB oscillations is nearly independent of field throughout the entire region of cyclotron resonance. One would expect that since the area of the classical cyclotron orbit decreases as the applied field increases, that the period of the AB oscillations might increase with increasing field. (Other unexpected features appear in this experiment which will not be treated in this Brief Report, but have been treated in detail elsewhere.<sup>4,5</sup>)

The reason the antidot experiment is a good example of the crossover region between the semiclassical and quantum transport regimes has to do with the interplay of the magnetic states—the classical cyclotron orbits—and the quantum-mechanical behavior enforced by the narrow constrictions. In previous work,<sup>4</sup> the transport coefficients were modeled numerically, and the qualitative behavior of the experiment was recovered. In addition, the decrease of the AB periods was shown to be qualitatively explained by considering Feynman path integrals of states enclosing the dots, which are constrained by hard walls at the channel edges.<sup>4</sup> The path-integral approach gives rise to stationary states which are qualitatively smaller than the classical cyclotron orbits for fields below resonance, because a vertical oval shape which just fits the constrictions has a larger net curvature than a circle which fits the constrictions. The oval “grows” with increasing field, until the cyclotron resonance, which accounts for the decrease in the AB period just below resonance. However, this picture breaks down at resonance, where purely quantum effects account for the field-independent AB period. Although a nearly constant AB period has been observed in other device geometries, the current device is most interesting to the crossover physics since the open channel allows the electron trajectories to be free to vary with magnetic field; in other devices, the constancy of the AB period was associated with geometric constraints on the electron trajectories, and the magnetic field simply provides a flux threading the fixed trajectories.<sup>8</sup> Also, many interesting collective effects, not associated with the free crossover from semiclassical to quantum ballistics, occur in arrays

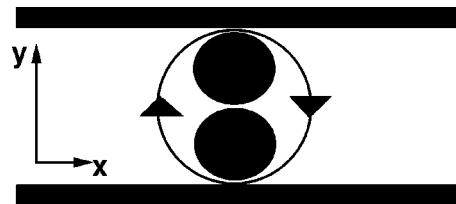


FIG. 1. The device geometry considered in this paper. The solid bars depict the gates defining the channel, while the solid circles depict the gates defining the antidots. The directed circular path is a schematic of a cyclotron orbit encircling the antidots.

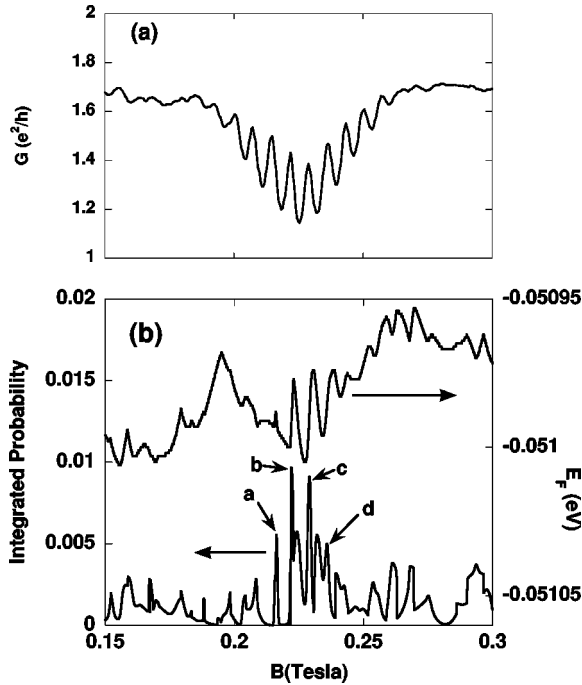


FIG. 2. (a) The experimental two-terminal conductance of the two-antidot device (from Ref. 3). (b) The integrated probability of the constriction region (left axis) for the calculated eigenstate at the Fermi level, and the Fermi level energy (right axis) as functions of magnetic field.

of antidots.<sup>9–12</sup> Other related experiments have been performed on arrays of quantum dots, but at very low temperatures, such that (periodic in the  $B$  field) oscillations arising via quantized orbits in antidot arrays appear in addition to the classical geometric effects of orbits which encompass fixed numbers of dots.<sup>13,14</sup> However, the study of the interplay of classical and quantum ballistics is much simpler in the geometry of the current paper; quantum-mechanical calculations for the potential landscape of the antidot arrays are too complex to distill the essential physics. However, the  $B$ -periodic conductance in these systems has been studied via trapped classical (chaotic) orbits.<sup>13</sup>

In this Brief Report, we study the stationary eigenstates of the device geometry themselves, as a function of applied magnetic field, to compare the spatial morphology of the states near the Fermi energy as a function of magnetic field. We will demonstrate that the system evolves from a more homogeneous, “classical” wave function to a sharply defined cyclotron orbitlike wave function, which then alternates at a roughly constant period with a low-conducting state associated with a “pinch-off” of the narrow constriction region between the antidots and the channel edges. This approach—the study of the stationary states of a closed model system—though not a transport model directly, nonetheless sheds light on the experimental results. Our picture may be thought of as an antidot pair strongly coupled to two very short leads with no voltage bias applied. In fact, we have run simulations of various sized “leads,” and the overall effects that we present in this paper are robust. The effects of the lead size may be broadly characterized as changing the

abruptness with which the state occupying the Fermi energy changes with the magnetic field. This will be explained further below.

The energy levels of the system evolve in a very complicated fashion as a function of field, i.e., the energy levels form an extraordinary web of level crossings. Therefore, the state occupying the Fermi energy is constantly changing. The web of level crossings is roughly analogous to the Darwin-Fock states associated with the parabolically confined (quantum dot) potential under an applied transverse magnetic field. In the Darwin-Fock case, the pattern of level crossings, and the corresponding jagged energy surface corresponding to the Fermi level, traces out a “devil’s staircase” fractal line.<sup>16</sup> States also pass through the Fermi level frequently as a function of field in the current model; near the cyclotron orbit, states of different morphology assume the Fermi level with a nearly constant period, a phenomenon closely related to the oscillations observed experimentally. The variation of the Fermi energy with constant period near the cyclotron resonance is independent of system size—it is therefore reasonable to assume that it occurs as well for open systems and does include the experimental results. As a result of the complex interplay between the semiclassical cyclotron orbit state and the fully quantum-mechanical effect of the narrow constrictions, we show that the conductance oscillations are not simple AB interference oscillations, but are also the result of states appearing at the Fermi energy which, as mentioned above, are “pinched off” in the constrictions, and result in a reflection of incident electrons. The transmission portion of the oscillation is due to the semiclassical cyclotron resonant state. Of course, AB interference is occurring for these states, as pointed out above, but it is the alternating appearance of the pinched-off (reflection) states and the cyclotron resonant states with a nearly fixed period in magnetic field which contributes most to the conductance oscillations.

The model that we utilize is a tight-binding Hamiltonian on a square lattice, which is diagonalized numerically. The Hamiltonian is given by

$$H = \sum_{m,n} a_{mn}^\dagger a_{mn} V_{mn} - t(a_{m+1n}^\dagger a_{mn} e^{i\theta} + a_{mn}^\dagger a_{m+1n} e^{-i\theta} + a_{mn+1}^\dagger a_{mn} + a_{mn}^\dagger a_{mn+1}). \quad (1)$$

The various components of this Hamiltonian are as follows:  $m$  and  $n$  are site labels in the  $x$  and  $y$  directions, respectively (see Fig. 1),  $t$  is the hopping energy given by  $\hbar^2/2m^*d^2$  (with  $d$  the lattice constant),  $\theta = eBd^2/\hbar$  is the magnetic phase associated with hopping in the  $x$  direction (we utilize the Landau gauge,  $\mathbf{A} = [-By, 0, 0]$ ),  $-e$  is the electron charge, and  $m^*$  is the electron effective mass. Also,  $V_{mn}$  is the potential energy of the site labeled  $m$  and  $n$ , and the device geometry is modeled via this term. We utilize the static potential model from Ref. 4, in which the lateral gates and the antidots are assumed to have parabolic potentials near their sides, with a flat potential elsewhere. Specifically,  $V(r) = (E_F/a^2)[r - a(1+s)]^2$  for  $r < a(1+s)$ , and  $V(r) = 0$  otherwise. Here  $r$  is the distance from the gate,  $a$  is a length scale (chosen to be  $0.05\mu$ ), and  $s$  is a dimensionless parameter which specifies the width of the depleted region

surrounding the gates themselves. By tuning the parameter  $s$ , the potential may be adjusted so that the system will transmit the proper number of modes through the constrictions.  $E_F$  is the Fermi energy for the two-dimensional system (measured from the bottom of the band). In our model, the square grid was  $170 \times 170$  sites, so 170 sites span the  $1 \mu$  sample; therefore the lattice constant  $d = 0.00588 \mu$ . Near the cyclotron resonance the magnetic field is roughly  $B = 0.23T$ , giving about nine lattice sites per magnetic length.

In Fig. 2(a), we show the experimental two-terminal conductance for the device depicted in Fig. 1 as a function of the applied magnetic field.<sup>3</sup> The conductance shows an overall dip, centered at the value of magnetic field where the cyclotron orbit of electrons in the two-dimensional gas “fit” between the channel boundaries and encircle the antidots (this orbit is depicted schematically in Fig. 1). The dip is modulated by oscillations with a nearly constant period. We note that in the experiment, the potential applied to the gates defining the anti-dots was tuned such that the constrictions between the antidots and the side gates admit one quantized transverse mode. For the calculations, we set the antidot gate parameter  $s = 2.05$ , such that the system admits a single transverse mode through the constrictions. [Hamiltonian (1) above was solved previously via different methods to establish the transport coefficients—see Ref. 4]. The constrictions between the antidots is pinched off. In Fig. 2(b), we show both the integrated probability in the constrictions and the Fermi level as functions of the applied magnetic field. The integrated probability is the sum of the modulus-squared eigenstates,  $|\psi_{nm}|^2$ , over the sites  $n$  and  $m$  that lie in the constrictions between the antidots and the side gates. The eigenstate used in the calculation is the Fermi level (explained below). The integrated probability calculation gives a very rough approximation of the behavior of the device conductance, since according to the two-terminal Landauer<sup>15</sup> formula the conductance is proportional to the transmission probability at the Fermi energy, and thus to the net probability to connect one side of a constriction to the other. The Fermi level is calculated by diagonalizing Hamiltonian (1) at a zero magnetic field, and the number of states between the bottom of the band and the Fermi energy is calculated. The Fermi level as a function of the applied field is then tracked by counting the same number of states from the bottom of the band at each magnetic field. The erratic traces of the Fermi level are the result of the many level crossings that occur as a function of magnetic field.

Several interesting features appear in Fig. 2(b). We note that the Fermi level shows a series of smooth transitions near the cyclotron resonance (which occurs at roughly  $0.225T$ ), with eigenstates being pushed through the Fermi energy at a *nearly constant period*, matching the period seen in the experimental conductance trace.<sup>17</sup> At the same time, significant spikes and dips appear in the integrated probability through the constrictions, also with the correct period. The combination of results—one from the overall magnetic dynamics and one from the role of the constrictions—indicates that the modulation of the conductance dip near the cyclotron reso-

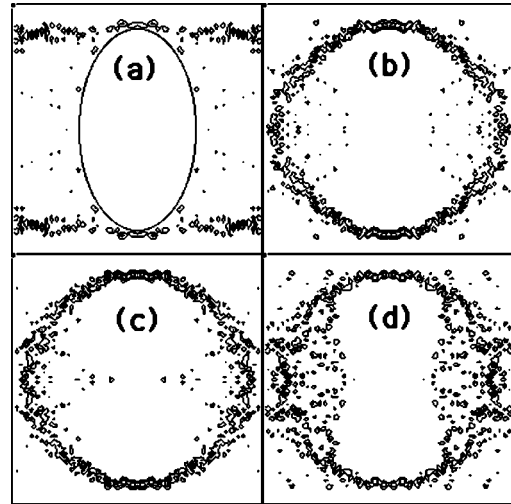


FIG. 3. Contour plots of the modulus-squared eigenstates corresponding to the labeled peaks in integrated probability from Fig. 2(b). Note that the peaks correspond to cyclotron-orbit-like states.

nance is significantly influenced by the complex interplay of the magnetic field dynamics and the quantization required by the constrictions.

To illustrate this interplay, Figs. 3(a)–3(d) show contour plots of the modulus-squared eigenstates of the system for the peaks labeled  $a$ – $d$  in Fig. 2(b). For clarity, we have chosen a very coarse contour plot utilizing only five contours, and thus the most important features show clearly. Note that the states associated with peaks  $b$  and  $c$  clearly show the cyclotron resonance, and so the cyclotron resonances are associated with a peak in conductance. Peak  $a$ , where the field is lower than the cyclotron field, is associated with a state resembling a “vertical oval.” The oval sketched on the figure corresponds to the stationary Feynman state at the appropriate magnetic field. Recall that the plot has only five contours, and thus the most prominent features are reflected; in the full eigenstate, the prominent peaks that lie on the oval state sketched in the figure are connected by smaller features. State  $d$ , on the other hand, is associated with a field higher than the cyclotron field, and shows the system’s attempt to accommodate a cyclotron orbit with a radius less than that which would “fit” into the constrictions. Note that the eigenstate is beginning to fill in the region around the antidots as the cyclotron orbit radius shrinks. It is important to reiterate that the system is changing from one eigenstate to another as the field is increased, and that states  $a$ – $d$  are not the same eigenstate.

Figure 4 illustrates the other types of eigenstates that appear. In (b) and (c), the states associated with the dramatic dips in integrated probability at  $B = 0.2184T$  and  $0.2272T$ , respectively, are shown. Note that the constrictions have been nearly pinched off for these states, corresponding to a conductance minimum; the oscillations in the conductance are associated with the alternating cyclotron-orbit-like states (relative maxima in conductance) with the near pinch-off of the constrictions (relative conductance minima), also occurring for states near the cyclotron resonance. The pinch-off is clearly an effect of states available in the constrictions at the

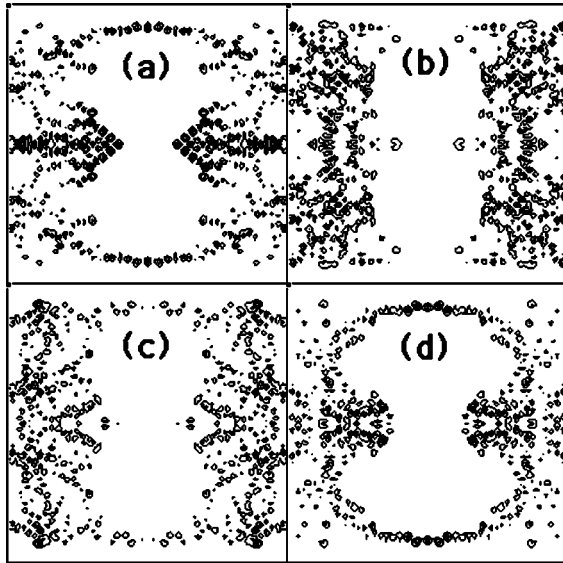


FIG. 4. (a) The modulus-squared eigenstate at zero magnetic field. This state corresponds to the single-mode conductance tuned at zero applied field. (b) and (c) The states corresponding to the minima in integrated probability at  $B=0.2184T$  and  $B=0.2272T$ , respectively. (d) The state at  $B=0.3836T$ , showing a return to single-mode transmission.

Fermi level, and is not associated directly with the semiclassical magnetic dynamics. It should be stressed that, due to the coarse contour plot, it artificially appears that  $|\psi|^2$  is zero in the constrictions, when it in fact is just very small.

For completeness, in Fig. 4(a) we show the eigensate at zero magnetic field; note that this picture corresponds to the

single-mode conductance of  $2e^2/h$  from the transport calculation, which, noting the relative “connectedness” of the two ends of the system via the eigenstate, lends plausibility to the argument for the integrated probability/conductance connection. In state *d*, the eigenstate at  $B=0.3836T$  is shown; this field is well above the conductance minimum, where the system has returned to the single-transmitted-mode regime. The state again shows that the two sample ends are well connected. Also, state *d* begins to depict the coming edge-state regime at higher fields, where the states are distributed in narrow regions near the sample boundaries and around the antidots.

In summary, we have calculated the eigenstates of the two-antidot system via a numerical diagonalization of a model potential, using standard techniques. The calculations shed light on the roles of the classical trajectories and the quantized motion of electrons through the narrow constrictions separating the antidots from the channel edges. We find that the conductance oscillations are due to the modulation of the state at the Fermi level with magnetic field, and that the morphology of the state occupying the Fermi level alternates smoothly between a conducting, cyclotron-orbit-like state and a nonconducting state with no appreciable contribution from the constriction. The modulation takes place at the same period as the experimental conductance oscillations, and is due to the complex level crossings associated with the simply-connected geometry.

#### ACKNOWLEDGMENTS

This work was supported by an award from Research Corporation.

<sup>1</sup>For reviews, see B.L. Johnson and G. Kirczenow, Rep. Prog. Phys. **60**, 889 (1997), or *The Quantum Hall Effect*, 2nd ed., edited by R.E. Prange and S.M. Girvin (Springer, New York, 1990).

<sup>2</sup>See S.E. Ulloa, A. MacKinnon, E. Castano, and G. Kirczenow in *Handbook of Semiconductors*, edited by P.T. Landesberg (North Holland, Amsterdam, 1992), Vol. 1.

<sup>3</sup>C. Gould, A.S. Sachrajda, Y. Feng, A. Delage, P.J. Kelly, K. Lung, and P.T. Coloeledge, Phys. Rev. B **51**, 11 213 (1995).

<sup>4</sup>G. Kirczenow, B.L. Johnson, P.J. Kelly, C. Gould, A.S. Sachrajda, Y. Feng, and A. Delage, Phys. Rev. B **56**, 7503 (1997).

<sup>5</sup>J. Blaschke and M. Brack, cond-mat/9906387 (unpublished).

<sup>6</sup>Y. Takagaki, Phys. Rev. B **55**, R16 021 (1997).

<sup>7</sup>C.C. Wan, T. De Jesus, and H. Guo, Phys. Rev. B **57**, 11907 (1998).

<sup>8</sup>G. Timp, A.M. Chang, J.E. Cunningham, T.Y. Chang, P. Mankiewich, R. Behringer, and R.E. Howard, Phys. Rev. Lett. **58**, 2814 (1987).

<sup>9</sup>E. Anisimovas and P. Johansson, Phys. Rev. B **60**, 7744 (1999).

<sup>10</sup>S. Uryu and T. Ando, Phys. Rev. B **65**, 035322 (2001).

<sup>11</sup>A.D. Chepelianskii and D.L. Shepelyansky, Phys. Rev. B **63**, 165310 (2001).

<sup>12</sup>P.H. Rivera, M.A. Andrade Neto, P.A. Schulz, and N. Studart, Phys. Rev. B **64**, 035313 (2001).

<sup>13</sup>D. Weiss, K. Richter, A. Menschig, R. Bergman, H. Schweizer, K. von Klitzing, and G. Weimann, Phys. Rev. Lett. **70**, 4118 (1993).

<sup>14</sup>K. Richter, Europhys. Lett. **29**, 7 (1995).

<sup>15</sup>For a review, see Y. Imry, in *Directions in Condensed Matter Physics*, edited by G. Grinstein and G. Masenko (World Scientific, Singapore, 1986), Vol. 1.

<sup>16</sup>B.L. Johnson and G. Kirczenow, Europhys. Lett. **51**, 367 (2000).

<sup>17</sup>The smooth transitions in the Fermi energy are one of the hallmarks of the results presented in this paper; the appearance of the smooth transitions occurs only near the cyclotron resonance, and is independent of the system size. Other simulations were run wherein the flat areas outside the antidot region were quite a bit larger (longer “leads”), and the same sort of behavior emerged, but with a lower resolution. The system size/geometry presented in this paper produced the clearest results.